THE
PHYSICS OF FLUIDS

VOLUME 3, NUMBER 6 NOVEMBER-DECEMBER, 1960

On Flow Duration in Low-Pressure Shock Tubes

ANATOL ROSHKO
Guggenheim Aeronautical Laboratory, California Institute of Technology, Pasadena, California
(Received June 9, 1960)

The severe decrease of flow duration in shock tubes operating at low pressures, previously reported by Duff, is confirmed by experiment and by an analysis of the effects of the laminar-boundary layer behind the shock wave. The latter leads to a shock tube similarity length parameter **X**, which depends on the tube pressure, diameter and shock Mach number, and to a flow duration parameter **T**. The theoretical relation $\mathbf{T} = \mathbf{T}(\mathbf{X})$ is determined and compared with experimental results. From the theoretical result $\mathbf{T}_{max} = 1$, the maximum possible flow duration τ_m in a shock tube is determined; it increases linearly with the initial pressure and the square of the tube diameter and decreases strongly with shock Mach number.

I. INTRODUCTION

IN THE theory of the ideal shock tube, the length l_i of the slug of shock-processed gas contained between the shock wave and contact surface (Fig. 1) satisfies the relation $\rho_2 l_i = \rho_1 x$, where x is the distance from the diaphragm to the shock position. That is, all the gas between the shock and the contact surface was initially between the position x and the diaphragm. Thus

$$l_i = x/\eta, \tag{1}$$

where

$$\eta = \rho_2/\rho_1.$$

Correspondingly, the ideal flow duration τ_i is given by $\tau_i = l_i/u_2$ (Fig. 1). The velocity u_2 of the shocked gas is related to the shock speed U_s by the continuity equation $\rho_2 u_2 = \rho_1(U_s - u_2)$, from which we have

$$u_2 = U_s(\eta - 1)/\eta. \tag{2}$$

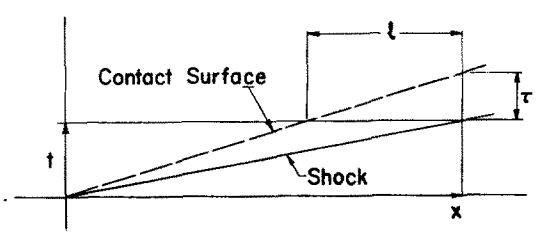

FIG. 1. x-t plane. l is the length of shocked gas. τ is the flow duration at x.

Combining this with Eq. (1), we obtain for the flow duration

$$\tau_i = x/[U_s(\eta - 1)],$$

or

$$\tau_i = x/a_1[M_s(\eta - 1)], \tag{3}$$

where a_1 is the speed of sound in the undisturbed gas and $M_s = U_s/a_1$ is the shock Mach number.

Values of flow duration, plotted in the dimensionless form $a_1\tau_i/x$ against M_s, are shown in Fig. 2, for air. The theoretical curves were obtained from Eq. (3), using values of the density ratio computed for constant specific heat and for real air.[1] The real-gas effect on the density ratio and thus on flow duration is appreciable.

Also shown in Fig. 2 are experimental values of $a_1\tau/x$, measured in a 2-in. diam. shock tube, 21 ft from the diaphragm. These measured values fall below even the theoretical real-gas curve; the discrepancy increases with increasing Mach number and decreasing initial pressure p_1

It has been well known that actual flow durations are shorter than the ideal values; a factor of one-half has been used as a rule of thumb which is useful at higher pressures (cf. Fig. 2 at $p_1 = 5$ mm). This loss of flow duration has been a point for con-

[1] S. Feldman, "Hypersonic gas dynamic charts," Avco Research Laboratory (1957).

Copyright © 1960 by the American Institute of Physics

Downloaded 14 Dec 2005 to 131.215.225.171. Redistribution subject to AIP license or copyright, see http://pof.aip.org/pof/copyright.jsp

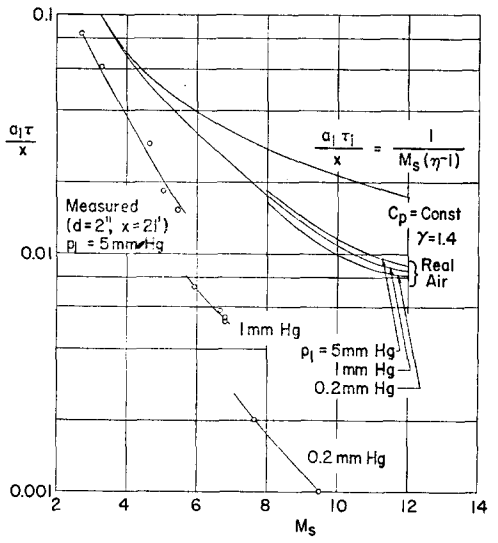

FIG. 2. Flow duration.

siderable speculation, it being usually attributed to effects connected with the nonideal diaphragm opening. At low values of p_1, the factor can actually be much less than one-half. The severe effect at low pressures was apparently first noted by Duff[2] who found that, at given p_1, there is, in fact, a limiting value of τ; i.e., τ cannot be increased by increasing x indefinitely. Duff gave a qualitative explanation of the loss, noting that the low speed gas in the boundary layer near the wall "leaks" past the contact surface.

In an apparently independent paper,[3] Anderson calculated the flow past the contact surface, obtaining some numerical results for a turbulent boundary layer, which gave $\tau/\tau_t = \frac{1}{2}$ for a typical case.

In the present paper we obtain some experimental and theoretical results for the flow duration at pressures low enough to ensure that the boundary layer is laminar. Our results appear to corroborate the effects which Duff described qualitatively and which seemed to be rather remarkable.

II. FLOW PAST THE CONTACT SURFACE

Figure 3 shows three coordinate systems from which the boundary layer behind the shock wave may be viewed. In the figure (a) shows the laboratory coordinates with shock wave moving at speed U_s, the fluid behind it moving at u_2, and velocity zero at the wall. The coordinate system in (b) is obtained from (a) by a velocity transformation which brings the shock wave to rest. This system, in which the boundary-layer flow is steady, is the one usually adopted for studying the shock tube boundary-layer problem. In Fig. 3 (c), which is obtained by another velocity transformation, the contact surface is at rest and the wall is moving past it with the speed u_2. Thus all the fluid in the boundary layer flows past the contact surface, from region 2 to region 3. It is this flow which accounts for the loss of shocked gas from region 2.

The mass flow past the contact surface in a tube of circular cross section[4] with diameter d may be written in the form,

$$\dot{m}_c = \pi d(\rho_w u_2\, \delta), \tag{4}$$

where ρ_w is the density at the wall, u_2 is the speed at the wall, and δ the mass flow thickness.

If the boundary layer is laminar, the thickness δ may be written in the form

$$\delta = \beta(\mu_w l/\rho_w u_2)^{\frac{1}{2}}, \tag{5}$$

where μ_w is the viscosity at the wall, corresponding to the wall temperature T_w, l is the development distance of the boundary layer, from shock wave to contact surface (Fig. 3), and β is a parameter which depends on conditions outside the boundary layer. Thus we have for the flow out of region 2, past the contact surface,

$$\dot{m}_c = \pi d\beta\rho_2 u_2 \frac{\rho_w}{\rho_2}\left(\frac{\mu_w l}{\rho_w u_2}\right)^{\frac{1}{2}}. \tag{6}$$

On the other hand the rate at which gas is being added to region 2 through the shock front [cf. Fig. 3(c)] is

$$\dot{m}_s = (U_s - u_2)\rho_2 \frac{\pi d^2}{4} = \frac{\rho_2 u_2}{\eta - 1}\frac{\pi d^2}{4}. \tag{7}$$

The mass between shock front and contact surface is increasing at the rate

$$\dot{m} = \dot{m}_s - \dot{m}_c, \tag{8}$$

where

$$\dot{m} = \rho_2 \frac{\pi d^2}{4}\dot{l}. \tag{9}$$

Putting relations (6), (7), and (9) into Eq. (8),

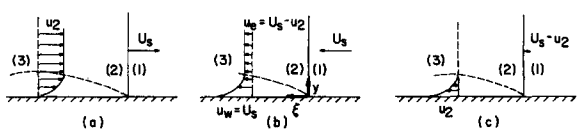

FIG. 3. Coordinate systems. (a) Shock tube system; gas in (1) at rest. (b) Shock wave at rest. (c) Contact surface at rest.

[2] R. E. Duff, Phys. Fluids 2, 207 (1959).
[3] G. F. Anderson, J. Aero/Space Sci. 26, 184 (1959).

[4] The final results are applicable also to a square tube of side d, since the ratio of cross-sectional to wetted area is the same as for the circular one.

Downloaded 14 Dec 2005 to 131.215.225.171. Redistribution subject to AIP license or copyright, see http://pof.aip.org/pof/copyright.jsp

we obtain, for the rate of increase of the length of region 2, the equation

$$\frac{dl}{dt} = \frac{u_2}{\eta - 1} - 4\beta \frac{\rho_w}{\rho_2} \frac{u_2}{d} \left(\frac{\mu_w}{\rho_w u_2}\right)^{\frac{1}{2}} l^{\frac{1}{2}}. \qquad (10)$$

III. SIMILARITY SOLUTION

The first term in Eq. (10) gives the ideal rate of increase of l, due to inflow at the shock front, while the second term is the loss due to leakage past the contact surface. We note that l reaches a maximum value l_m when $dl/dt = 0$. Setting the right-hand side of Eq. (10) equal to zero, we find

$$l_m = \frac{1}{16\beta^2} \left(\frac{\rho_2}{\rho_w}\right)^2 \frac{d^2}{(\eta - 1)^2} \frac{\rho_w u_2}{\mu_w} \qquad (11)$$

and then rewrite Eq. (10) in the form

$$\frac{dl}{dt} = \frac{u_2}{\eta - 1} [1 - (l/l_m)^{\frac{1}{2}}]$$

or

$$\frac{d(l/l_m)}{d[u_2 t/(\eta - 1) l_m]} = 1 - \left(\frac{l}{l_m}\right)^{\frac{1}{2}}.$$

The variables in the last equation may be identified as follows:

$$\frac{l}{l_m} = \frac{\tau}{\tau_m} \equiv \mathbf{T}, \qquad (12)$$

$$\frac{u_2 t}{(\eta - 1) l_m} = \frac{U_s t}{\eta l_m} = \frac{x}{\eta l_m} \equiv \mathbf{X}. \qquad (13)$$

Thus $\mathbf{T}$ is the dimensionless flow duration and $\mathbf{X}$ the dimensionless distance of the shock wave from the diaphragm. These are actually similarity parameters, and the differential equation now reduces to the form

$$d\mathbf{T}/d\mathbf{X} = 1 - \mathbf{T}^{\frac{1}{2}}. \qquad (14)$$

In the corresponding equation for an ideal shock tube, the second (leakage) term is absent and then

$$d\mathbf{T}_i/dX = 1, \quad \text{or} \quad \mathbf{T}_i = \mathbf{X},$$

while for the viscous case we have, from the solution of Eq. (14),

$$\mathbf{X}/2 = -\ln (1 - \mathbf{T}^{\frac{1}{2}}) - \mathbf{T}^{\frac{1}{2}}. \qquad (15)$$

In these similarity parameters the maximum testing time is

$$\mathbf{T}_m = 1$$

which is reached asymptotically as $\mathbf{X} \to \infty$.

Equation (15) is plotted in Fig. 4, and the ideal testing time is shown for comparison. It may be seen that at $\mathbf{X} = 1$, $\mathbf{T}/\mathbf{T}_i \doteq 0.5$, while at $\mathbf{X} = 10$, $\mathbf{T}/\mathbf{T}_i \doteq 0.1$.

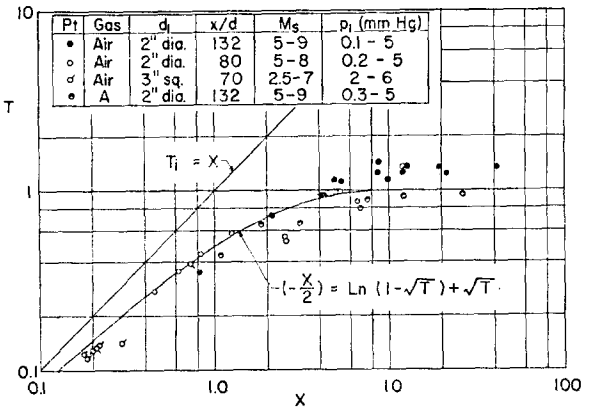

FIG. 4. Plot of theory and data in similarity parameters.

We now have to identify the similarity parameters in terms of the real variables of the problem. From Eqs. (13) and (11),

$$\mathbf{X} = 16\beta^2 \left(\frac{\rho_w}{\rho_2}\right)^2 \frac{(\eta - 1)^2}{\eta} \frac{\mu_w}{\rho_w u_2} \frac{x}{d^2}.$$

Noting that

$$\rho_w = (\rho_w/\rho_2)\eta\rho_1$$

$$u_2 = U_s(\eta - 1)/\eta = M_s a_1(\eta - 1)/\eta$$

$$\mu_w \doteq \mu_1, \text{ since } T_w \doteq T_1,$$

we have

$$\mathbf{X} = 16\beta^2 \frac{\rho_w}{\rho_2} \frac{\eta - 1}{\eta} \frac{\mu_1}{\rho_1 a_1 M_s} \frac{x}{d^2}.$$

Finally, if we introduce standard (room temperature and atmospheric pressure) values of viscosity, μ_s, ρ_s, p_s, etc. and assume that the initial temperature $T_1 = T_s$, we have $\mu_1 = \mu_s$, $a_1 = a_s$, $\rho_1 = (\rho_1/\rho_s)\rho_s = (\rho_1/\rho_s)\rho_s$. Therefore,

$$\mathbf{X} = 16\left(\frac{\mu}{\rho a}\right)_s \beta^2 \frac{\rho_w}{\rho_2} \frac{\eta - 1}{\eta} \frac{1}{M_s} \frac{p_s}{p_1} \frac{x}{d^2}. \qquad (16)$$

To write out $\mathbf{T} \equiv \tau/\tau_m = l/l_m$ we note that $l = u_2\tau = U_s\tau(\eta - 1)/\eta = M_s a_1 \tau(\eta - 1)/\eta$ and that $l_m = x/(\eta\mathbf{X})$ [cf. Eq. (13)]. Thus

$$\mathbf{T} = \mathbf{X}(\eta - 1)M_s(a_1\tau/x). \qquad (17)$$

The ratio ρ_w/ρ_2 which appears in the expressions for $\mathbf{X}$ and $\mathbf{T}$ is the density ratio across the boundary layer. Since the pressure across the boundary layer is constant, we may write

$$\frac{\rho_w}{\rho_2} = \frac{1}{Z_2} \frac{T_2}{T_w} \doteq \frac{1}{Z_2} \frac{T_2}{T_1}, \qquad (18)$$

Downloaded 14 Dec 2005 to 131.215.225.171. Redistribution subject to AIP license or copyright, see http://pof.aip.org/pof/copyright.jsp

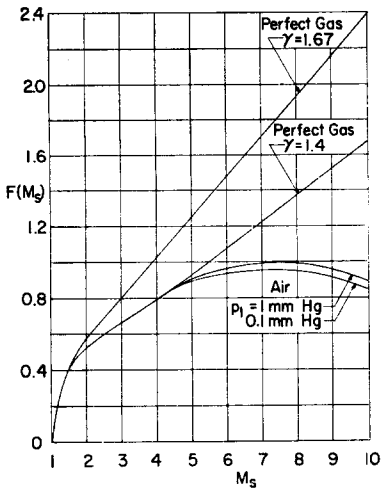

FIG. 5. The function $F(M_s) = \frac{1}{Z_2}\frac{T_2}{T_1}\frac{\eta - 1}{\eta}\frac{1}{M_s}$.

where Z is the compressibility factor (1 for a perfect gas) and T_2/T_1 is the temperature ratio across the shock. We may now express the shock parameters in the form

$$F(M_s) = \frac{1}{Z_2}\frac{T_2}{T_1}\frac{\eta - 1}{\eta}\frac{1}{M_s} \tag{19a}$$

$$G(M_s) = \frac{1}{Z_2}\frac{T_2}{T_1}\frac{(\eta - 1)^2}{\eta} \tag{19b}$$

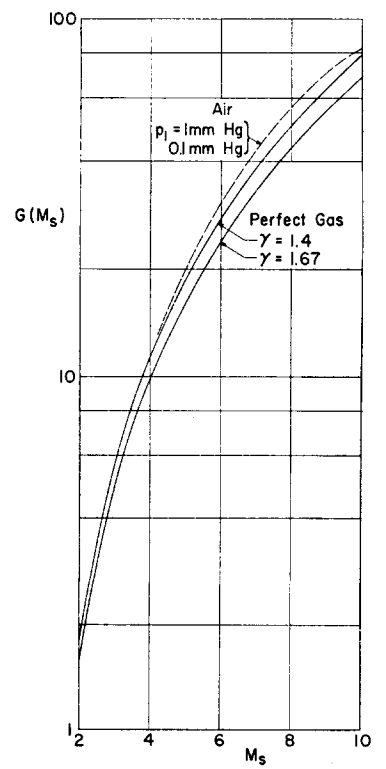

FIG. 6. The function $G(M_s)$.

and write the similarity parameters

$$\mathbf{X} = 16\left(\frac{\mu}{\rho a}\right)_s \beta^2 F(M_s)\frac{p_s}{p_1}\frac{x}{d^2} \tag{20}$$

$$\mathbf{T} = 16\left(\frac{\mu}{\rho a}\right)_s \beta^2 G(M_s)\frac{p_s}{p_1}\frac{a_1 \tau}{d^2}. \tag{21}$$

$F(M_s)$ and $G(M_s)$ are plotted in Figs. 5 and 6.

IV. THE PARAMETER β

The boundary layer parameter β introduced in the definition of mass flow thickness [Eqs. (4) and (5)] will be a function of the Mach number M_2 of the flow behind the shock and of the temperature ratio ($T_2/T_w \doteq T_2/T_1$) across the boundary layer. Thus it is indirectly also a function of the shock Mach number M_s. In the later paragraphs we shall discuss some attempts to evaluate it. For the present, we assume it to be a constant, fitted to the experimental data.

Choosing $\beta = \sqrt{3}$ and using Eqs. (20) and (21) to evaluate $\mathbf{X}$ and $\mathbf{T}$ from measurements in shock tubes we obtain the experimental points shown plotted in Fig. 4. They were obtained by the method described next.

V. SHOCK TUBE MEASUREMENTS

In his experimental results, Duff[2] used an electron beam to detect the passage of shock wave and contact surface, and thus measured the flow duration.

In our experiments we used a fine wire, arranged like a standard hot-wire anemometer normal to the flow direction, to detect the passage of the shock wave and contact surface. The constant current through the wire is low and does not heat the wire appreciably. When the shock passes, the wire suddenly finds itself in the hot flow in region 2 and begins to heat up. With uniform conditions in region 2 the heat transfer rate to the wire is constant and thus the wire temperature rises uniformly.[5] The resulting wire resistance changes are translated into a voltage signal, in the usual way, and recorded on an oscillograph. An example is shown in Fig. 7 on which the uniform temperature rise time between shock arrival and contact surface arrival are clearly visible. More complete details of this use of fine wire calorimeters in shock tubes are reported elsewhere.[6]

A few determinations of contact surface arrival

[5] In this statement we are neglecting the fact that the temperature loading ($T_e - T_{wire}$) decreases as the wire temperature rises; for strong shocks the wire heats up to only a fraction of its equilibrium value T_e, and thus the heat transfer rate is practically constant.

[6] Walter H. Christiansen, Phys. Fluids **3**, 1027(1960).

Downloaded 14 Dec 2005 to 131.215.225.171. Redistribution subject to AIP license or copyright, see http://pof.aip.org/pof/copyright.jsp

were also obtained by means of a stagnation point heat transfer gauge, a technique that is well known in shock tube work. These agree with the fine wire measurements; the fine wire technique, however, can be used down to much lower pressures.

The experiments were made in the 2-in. diam and 3-in. sq shock tubes at this Laboratory. Measurements were obtained at several distances from the diaphragm, up to 23 ft; shock speeds were determined in a conventional way, using thin-film resistance gauges on the side wall and an electronic chronometer to measure the time of passage over a known length. Driver gases were nitrogen and helium, driven gases were air and argon, initial pressures had values between 0.1 and 10 mm Hg. The round tube has a leakage rate of 6 μ Hg/hr, ensuring that the low pressures can be accurately determined and that there is no leakage contamination in the argon experiments. Shock Mach numbers varied from 2.5 to 9; the higher Mach numbers were obtained with the help of an electric heater in the driver of the round tube.

For reducing the measurements into similarity form, we found it convenient to write Eqs. (20) and (21) in the form[7]

$$\mathbf{X} = AF(M_s)\, x/(p_1 d^2) \tag{22}$$

$$\mathbf{T} = AG(M_s)\, a_1\tau/(p_1 d^2), \tag{23}$$

where $A = 16(\mu/\rho a)_s\beta^2 p_s = 0.0650$ for air and 0.0623 for argon if p_1 is measured in millimeters of Hg, d in inches, and $\beta^2 = 3$.

VI. THE MAXIMUM FLOW DURATION

The maximum value of the similarity parameter $\mathbf{T}_m = 1$. Therefore, from Eq. (21) we have for the maximum flow duration

$$\tau_m = \left[16\left(\frac{\mu}{\rho}\right)_s \beta^2 p_s\right]^{-1} \frac{p_1 d^2}{G(M_s)}. \tag{24}$$

The maximum flow duration is proportional to the initial pressure in the tube, as found experimentally by Duff,[2] and to the square of the diameter, as had been inferred by Duff. In addition it decreases rapidly with shock Mach number, since $G(M_s)$ increases rapidly with M_s (Fig. 6). The Mach number effect is considerably greater than for the ideal shock tube (Fig. 3), the greater effect being due to the fact that the density ratio across the boundary layer and thus the density near the cool wall, as well as the leakage velocity, increase with M_s.

[7] One can also compute **T** conveniently from Eq. (17).

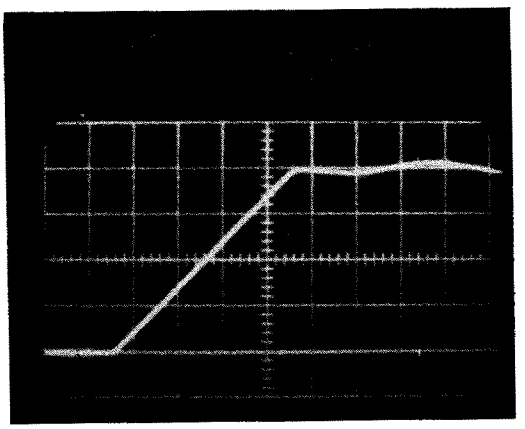

FIG. 7. Oscillogram of output from 0.0006-in. tungsten wire probe. $M_s = 5.35$; $p_1 = 3$ mm Hg; horizontal sweep 50 μsec/division; vertical sweep 5 mv/division; voltage across wire 12.5 mv.

If p_1 is measured in millimeters of Hg, d in inches, and τ in milliseconds, then Eq. (24) may be written

$$\begin{aligned} \tau_m &= 1.13 p_1 d^2/G \quad \text{for air,} \\ \tau_m &= 1.27 p_1 d^2/G \quad \text{for argon.} \end{aligned} \tag{25}$$

From a comparison with the experimental results in Fig. 4, it appears that these formulas will be conservative for air and slightly nonconservative for argon.

VII. MAXIMUM TUBE LENGTH

The maximum flow duration $\tau_m(\mathbf{T} = 1)$ is attained at $\mathbf{X} = \infty$, but 90% of it ($\mathbf{T} = 0.9$) is attained already at $\mathbf{X} = 4$. Taking this as the criterion for tube length, we obtain from Eq. (22) the corresponding tube length

$$x_0 = 4\, p_1 d^2/(AF).$$

With p_1 in millimeters Hg and d in inches, the expression becomes

$$\begin{aligned} x_0/d &= 62\, p_1\, d/F(M_s) \quad \text{for air,} \\ x_0/d &= 64\, p_1\, d/F(M_s) \quad \text{for argon.} \end{aligned} \tag{26}$$

For given conditions, there is little to be gained by making the tube longer than x_0. (Obviously, in practice, there is a lower limit on x_0/d which is determined by other considerations, e.g., the distance required for the shock to develop.)

VIII. BOUNDARY LAYER THICKNESS

The maximum value which the mass flow thickness δ can attain in region 2 may be calculated by putting l_m in Eq. (5):

$$\delta_m = \beta\left(\frac{\mu_w l_m}{\rho_w u_2}\right)^{\frac{1}{2}}.$$

Downloaded 14 Dec 2005 to 131.215.225.171. Redistribution subject to AIP license or copyright, see http://pof.aip.org/pof/copyright.jsp

With Eq. (11) for l_m, this becomes

$$\frac{\delta_m}{d} = \frac{1}{4}\frac{T_1}{T_2}\frac{1}{\eta - 1}. \tag{27}$$

Except for very weak shocks (i.e., $\eta - 1 < 1$), the value of δ_m/d is small. This is a consequence of the fact that (i) the density near the wall is high and (ii) the growth of the layer is limited by the limited growth of region 2.

For estimating the effect of the boundary layer on density measurements which utilize a beam that traverses the tube, we note that in the ideal case the mass traversed by unit area of the beam would be $\rho_2 d$, but because of the boundary layer the additional mass seen by the beam is $(\rho_w - \rho_2)/(2\delta)$. Thus the fractional increase in mass seen by the beam is

$$\Delta m/m = 2[(\rho_w/\rho_2) - 1]\ \delta/d.$$

Using Eq. 5 for δ, and rearranging, we find

$$\frac{\Delta m}{m} = 2\beta\left[\frac{(T_2/T_1 - 1)^2}{(T_2/T_1)M_s(\eta - 1)}\right]^{\frac{1}{2}}\left(\frac{\mu_1}{\rho_1 a_1}\right)^{\frac{1}{2}}\frac{(\xi)^{\frac{1}{2}}}{d}, \tag{28}$$

where ξ is the distance behind the shock wave. If $T_w = T_1 = T_s$, p_1 is measured in millimeters of Hg and ξ and d in inches, we can put $2\beta(\mu_1/\rho_1 a_1)^{\frac{1}{2}} = \frac{1}{2}(A/p_1)^{\frac{1}{2}}$, where A is given in Sec. V.

IX. EVALUATION OF β FROM MIRELS' SOLUTION

To obtain a better estimate of β we need the velocity and density profiles in the boundary layer, in order to evaluate the mass flow integral

$$\dot{m}_c = \pi d\int_0^\infty \rho u\, dy.$$

This integral is written in contact surface coordinates [Fig. 3(c)]; it is convenient to rewrite it in shock coordinates [Fig. 3(b)] in which system the boundary layer flow is steady. The result is

$$\dot{m}_c = \pi d\int (\rho u - \rho_2 u_e)\, dy. \tag{29}$$

Several authors have obtained solutions of the shock tube boundary layer problem, all of them limited by various assumptions. Probably the most complete solutions are those given by Mirels.[8] He makes the following assumptions: Prandtl number is unity, $\mu \sim T$; the gas is perfect. Introduction of the Howarth-Dorodnitzyn similarity transformation,

$$\rho\, dy = \rho_w(2\mu_w\xi/\rho_w u_e)^{\frac{1}{2}}\, d\zeta \tag{30}$$
$$u/u_e = f'(\zeta),$$

leads to total differential equations for $f(\zeta)$, which were solved on an electronic computer.[8]

To make use of Mirels' solution, we introduce the transformation (30) in Eq. (29), which becomes

$$\dot{m}_c/\pi d = \rho_w u_e\left(\frac{2\mu_w\xi}{\rho_w u_e}\right)^{\frac{1}{2}}\int_0^\infty f'(\zeta)\, d\zeta - \rho_e u_e y_\infty. \tag{31}$$

Mirels' solution leads to an expression for y_∞:

$$y_\infty = \frac{T_2}{T_w}\left(\frac{2\mu_w l}{\rho_w u_e}\right)^{\frac{1}{2}} \cdot\left\{\zeta_\infty + \left(\frac{T_w}{T_2} - 1\right)(f_\infty - \zeta_\infty)\Big/\left\{\frac{u_s}{u_e} - 1\right\} + \frac{\gamma - 1}{2}M_e^2\left[\frac{u_s}{u_e}(f_\infty - \zeta_\infty) + f''(0)\right]\right\}.$$

With this in Eq. (31), and noting that $u_s/u_e = \eta$, $T_w \doteq T_1$, comparison with Eq. (6) leads to

$$\beta = \left(\frac{2}{\eta - 1}\right)^{\frac{1}{2}}\left[(f_\infty - \zeta_\infty)\left(1 + \frac{1 - T_1/T_2}{\eta - 1} - \frac{\gamma - 1}{2}M_e^2\eta\right) - \frac{\gamma - 1}{2}M_e^2 f''(0)\right]. \tag{32}$$

The difference $(f_\infty - \zeta_\infty)$ is finite, and may be obtained together with $f''(0)$ from the tables of solutions in reference 8. The results, for the values of η tabulated there, are given in Table I and may be compared to our empirically chosen constant value, $\beta = \sqrt{3} = 1.73$.

TABLE I.

η	1.5	2	3	4	5	6
M_s	1.29	1.58	2.24	3.16	5.00	∞
β	0.91	1.13	1.33	1.42	1.42	1.52

[8] H. Mirels, National Advisory Committee for Aeronautics, Tech. Note 3401 (1955).

X. AN INTEGRAL SOLUTION

If we introduce the Crocco transformation

$$dy = \mu\, du/\tau,$$

where τ is the shearing stress, then the mass flow integral, Eq. (28), may be expressed in the form

$$\frac{\dot{m}_c}{\pi d} = \int_{u=0}^{u=u_2}\rho u\frac{\mu}{\tau}\, du = \frac{\rho_w\mu_w}{\tau_w}u_2^2\int_0^1\frac{\psi}{g}\lambda\, d\lambda, \tag{33}$$

where

$$\lambda = u/u_2;\quad \psi(\lambda) = \rho\mu/(\rho\mu)_w;\quad g(\lambda) = \tau/\tau_w. \tag{34}$$

We now have to make some assumptions about ψ and g. We will assume that ψ is linear with respect to λ and that g varies as $\lambda^{\frac{1}{2}}$:

$$\psi(\lambda) = \psi_2 + (1 - \psi_2)\lambda;\qquad g(\lambda) = \lambda^{\frac{1}{2}}, \tag{35}$$

Downloaded 14 Dec 2005 to 131.215.225.171. Redistribution subject to AIP license or copyright, see http://pof.aip.org/pof/copyright.jsp

where

$$\psi_2 = \frac{\rho_2\mu_2}{\rho_w\mu_w} = \frac{T_w\mu_2}{T_2\mu_1} = \frac{T_1}{T_2}\frac{\mu_2}{\mu_1}. \tag{36}$$

Putting these assumed forms into Eq. (33), we get

$$\dot{m}_c/\pi d = \frac{2}{15}(3 + 2\psi_2)\frac{\rho_w\mu_w}{\tau_w}u_2^2. \tag{37}$$

It is now necessary to evaluate τ_w for the assumed profiles of g and ψ. This can be accomplished by starting with the well-known integral expression, written for the steady flow coordinate system [Fig. 3(b)],

$$\tau_w = \frac{d}{d\xi}\int_0^\infty \rho u(u_e - u)\,dy$$

and using the Crocco transformation to rewrite it in the form

$$\tau_w = \rho_w\mu_w u_e^3 \frac{d}{d\xi}\left[\frac{1}{\tau_w}\int_1^{u_w/u_e}\frac{\psi}{g}(\sigma - 1)\sigma\,d\sigma\right], \tag{38}$$

where $\sigma = u/u_e$, $\psi(\sigma) = \rho\mu/(\rho\mu)_w$, and $g(\sigma) = \tau/\tau_w$. We again assume linear and square root functions, respectively,

$$\psi(\sigma) = \psi_2 + (1 - \psi_2)(\sigma - 1)/(\eta - 1);$$

$$g(\sigma) = [(\sigma - 1)/(\eta - 1)]^{\frac{1}{2}}.$$

With these, and noting that $u_w/u_e = \eta$, we can evaluate the integral, which we call α:

$$\alpha = \frac{2}{105}(\eta - 1)^2[\eta(15 + 6\psi_2) + 6 + 8\psi_2].$$

Solution of the differential equation, Eq. (38), integrating from $\xi = 0$ to $\xi = l$, then gives

$$\tau_w = (\alpha\rho_w\mu_w u_e^3/2l)^{\frac{1}{2}}$$

which in Eq. (37) leads to

$$\dot{m}_c/\pi d = \frac{2}{15}\left(\frac{2}{\alpha}\right)^{\frac{1}{2}}(3 + 2\psi_2)\left(\frac{u_2}{u_e}\right)^{\frac{3}{2}}\rho_w u_2(\mu_w l/\rho_w u_2)^{\frac{1}{2}}.$$

On comparing with Eq. (6) and noting that $u_2/u_e = \eta - 1$, it is seen that

$$\beta^2 = \frac{28}{15}\frac{(\eta - 1)(3 + 2\psi_2)^2}{\eta(15 + 6\psi_2) + 6 + 8\psi_2}. \tag{39}$$

To estimate the accuracy of the integral method, we can compare with Mirels' exact solution, in which it was assumed that $\mu \sim T$. In our results this corresponds to $\psi_2 = 1$, and then Eq. (39) reduces to

$$\beta^2 = (20/3)[(\eta - 1)/(3\eta + 2)]. \tag{40}$$

For the values of η computed by Mirels we obtain the results in Table II, and compare them with Mirels' values from Table I. The integral method gives consistently low values. Other choices of fitting curve for g were tried. A quadratic gives nearly the same results as Eq. (40), while a linear curve gives values somewhat higher than the exact values of β. We did not investigate the effect of choosing other than linear variations for ψ.

TABLE II.

η	1.5	2	3	4	5	6
β [Eq. (40)]	0.72	0.91	1.10	1.20	1.25	1.29
β (Table I)	0.91	1.13	1.33	1.42	1.42	1.52

To estimate the effect of the viscosity law, the Sutherland law was used to evaluate ψ_2 in Eq. (39). The results are shown in Table III for perfect air ($\gamma = 1.4$) and argon ($\gamma = 1.67$). With real gas values for η and the Sutherland formula for viscosity, the results for air are as shown in Table IV. If the trend for the real gas values is the same as for the case in Table II, then we could expect an exact solution to give higher value of β than those in Table IV, but whether they would be as high as our empirical value $\sqrt{3}$ is not clear.

TABLE III.

M_s	2	4	6	8	∞
β (air)	1.02	1.11	1.09	1.09	0.94
β (argon)	0.94	1.02	1.00	0.97	0.88

TABLE IV.

M_s	2	4	6	8	10
β (p_1 = 1 mm)	1.02	1.13	1.13	1.14	1.15
β (p_1 = 0.1 mm)	1.02	1.13	1.13	1.15	1.22

XI. EFFECT OF SHOCK ATTENUATION

In our calculations of flow duration, the boundary layer has been calculated for constant shock speed and constant conditions in region 2, i.e., as if the shock motion were given by the ideal theory. However, the loss of gas from this region affects the motion of the shock relative to the contact surface; the shock speed U_s must tend toward the contact surface speed u_2. In the ideal case, with no loss of gas, we have $U_s/u_2 = \eta/(\eta - 1)$, Eq. (2), while in the limiting case, when $\tau = \tau_m$, we have $U_s/u_2 = 1$. If η is large, as for strong shocks in air, these two values do not differ much and thus the decrease in

Downloaded 14 Dec 2005 to 131.215.225.171. Redistribution subject to AIP license or copyright, see http://pof.aip.org/pof/copyright.jsp

shock speed cannot be large (neglecting possible viscous effects on the driver gas). At low shock Mach numbers, the difference is appreciable, and neglect of the shock deceleration will lead to appreciable error in the estimate of flow duration.

In a given case it may be possible to compute the boundary layer development correctly, simultaneously with the changing shock speed and changing conditions in region 2, but it will probably be too complicated to enable general conclusions to be drawn. Instead we shall attempt to estimate the effect as follows.

Suppose that at the test station the flow duration has reached its maximum value τ_m. Then $U_s = u_2$, and $u_2/a_1 = U_s/a_1 = M_s$. Assuming that u_2 is constant from the beginning of the motion, we can compute the shock Mach number M_{s_0} at the beginning, when no leakage has yet occurred. This is given by

$$M_{s_0}(\eta_0 - 1)\eta_0 = u_2/a_1 = M_s. \tag{41}$$

This establishes a definite relation between the Mach number M_s at the limiting condition and the corresponding initial value M_{s_0}. Typical values are given in Table V.

Now the values of τ_m and l_m obtained by previous considerations will be too high because the leakage rate $\dot{m}_c$ was written for constant M_s, whereas in fact the values of M_s and correspondingly of $\dot{m}_c$ are higher in the earlier portions of the motion. For a lower limit on τ_m we could calculate τ_m for M_{s_0} instead of the observed value M_s, i.e., use $G(M_{s_0})$ instead of $G(M_s)$ in Eqs. (24) and (25). The resulting estimates for τ_m should be conservative.

In obtaining Eq. (41) we have assumed constant u_2, but in fact it will be changing since the driver gas must adjust itself to a changing pressure p_2. The correct computation can be easily carried out, but the result then depends on the driver gas. For example, one can solve the shock tube equation for the condition[9] $u_2 = U_s$, compare it with the ideal equation, and thus find a correspondence between M_{s_0} and M_s. The simpler results of Eq. (41) will serve for the estimate we require.

TABLE V.

M_s	1.5	2	3	4	6	8	10
M_{s_0}							
air (p_1 = 1 mm)	2.32	2.76	3.86	4.91	6.97	8.97	11.00
argon (γ = 1.67)	2.41	3.00	4.24	5.51	8.12	10.75	13.40

[9] The result is nearly the same as the modified shock tube equation obtained by Duff with a somewhat different assumption.

XII. CONCLUDING REMARKS

The main assumptions made in deriving the similarity law and in plotting the experimental data to fit it were the following: (a) constant M_s; (b) constant β; (c) no relaxation effects. Of these the first seems to be the most serious, and we have tried to obtain an estimate of its effects in the preceding article. We may note that most of our data are for high values of M_s, for which the effect in air is not too serious. It probably accounts also for the systematic discrepancy between the asymptotic behavior of the plotted values for air and argon (Fig. 4).

We have not settled the question of how closely our empirical value of β would agree with an exact computation, using a correct viscosity law. The indications are that the empirical value is a little high; the effect described in the preceding article would tend to make it so. Furthermore, β will not actually be a constant with respect to M_s, γ, real-gas effects, etc. However, until account is taken of the effects mentioned in the preceding article, we feel that the simplifications introduced are reasonable, and they lead to a fairly simple law for estimating the effects of pressure, M_s, and tube diameter on flow duration.

We may conclude that the loss of flow duration at low pressures is due mainly to the loss of shocked gas by leakage of the boundary layer past the contact surface, as proposed by Duff and independently by Anderson. An alternative picture is to regard the wall as a sink (the displacement thickness is negative). We may also conclude with Duff that the deceleration of the shock wave toward the contact surface plays an important role in its over-all deceleration.

Care must be exercised in interpreting the results of experiments carried out in small shock tubes at low pressure, practicularly with strong shock waves, as is now the fashion. All three factors contribute to a decrease of flow duration and of distance between shock wave and contact surface; these may become vanishingly small!

Finally, the mass accumulation on the walls must be taken into account in density measurements which utilize a traversing beam.

ACKNOWLEDGMENT

This work was carried out under the sponsorship and with the financial assistance of the Office, Chief of Ordnance, and the Office of Ordnance Research, U. S. Army.

Downloaded 14 Dec 2005 to 131.215.225.171. Redistribution subject to AIP license or copyright, see http://pof.aip.org/pof/copyright.jsp